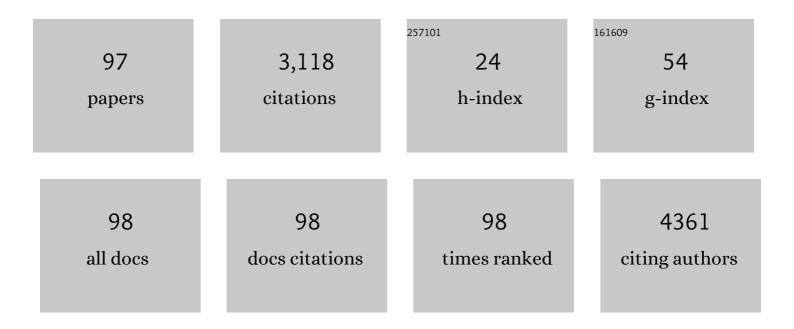
## Hieu T Nguyen

List of Publications by Year in descending order

Source: https://exaly.com/author-pdf/7978988/publications.pdf Version: 2024-02-01



#	Article	IF	CITATIONS
1	Origin of Efficiency and Stability Enhancement in Highâ€Performing Mixed Dimensional 2Dâ€3D Perovskite Solar Cells: A Review. Advanced Functional Materials, 2022, 32, 2009164.	7.8	96
2	Electrical properties of perovskite solar cells by illumination intensity and temperatureâ€dependent photoluminescence imaging. Progress in Photovoltaics: Research and Applications, 2022, 30, 1038-1044.	4.4	7
3	Tuning the crystal structure and optical properties of selective area grown InGaAs nanowires. Nano Research, 2022, 15, 3695-3703.	5.8	5
4	All room-temperature synthesis, N2 photofixation and reactivation over 2D cobalt oxides. Applied Catalysis B: Environmental, 2022, 304, 121001.	10.8	11
5	Interfacing transition metal dichalcogenides with chromium germanium telluride quantum dots for controllable light-matter interactions. Journal of Colloid and Interface Science, 2022, 611, 432-440.	5.0	2
6	Photoluminescence Spectroscopy of Thermal Donors and Oxygen Precipitates Formed in Czochralski Silicon at 450 °C. IEEE Journal of Photovoltaics, 2022, 12, 222-229.	1.5	1
7	Comparison of firing stability between p―and nâ€ŧype polysilicon passivating contacts. Progress in Photovoltaics: Research and Applications, 2022, 30, 970-980.	4.4	10
8	Effective Passivation of InGaAs Nanowires for Telecommunication Wavelength Optoelectronics. Advanced Optical Materials, 2022, 10, .	3.6	5
9	Nanoscale localized contacts for high fill factors in polymer-passivated perovskite solar cells. Science, 2021, 371, 390-395.	6.0	270
10	Highly Enhanced Light–Matter Interaction in MXene Quantum Dots–Monolayer WS <sub>2</sub> Heterostructure. Small, 2021, 17, e2006309.	5.2	22
11	Morphology, microstructure, and doping behaviour: A comparison between different deposition methods for polyâ€6i/SiO <sub><i>x</i></sub> passivating contacts. Progress in Photovoltaics: Research and Applications, 2021, 29, 857-868.	4.4	16
12	Boron Spin-On Doping for Poly-Si/SiO <sub><i>x</i></sub> Passivating Contacts. ACS Applied Energy Materials, 2021, 4, 4993-4999.	2.5	9
13	Understanding the Role of Vanadium Vacancies in BiVO <sub>4</sub> for Efficient Photoelectrochemical Water Oxidation. Chemistry of Materials, 2021, 33, 3553-3565.	3.2	54
14	Comparative studies of optoelectronic properties, structures, and surface morphologies for phosphorus-doped poly-Si/SiOx passivating contacts. , 2021, , .		0
15	Mechanisms of luminescence in silicon photovoltaics. , 2021, , .		0
16	Imaging pseudo current-voltage characteristics of perovskite solar cells using Suns-photoluminescence. , 2021, , .		1
17	Firing Stability of Polysilicon Passivating Contacts: The Role of Hydrogen. , 2021, , .		5
18	Contactless and Spatially Resolved Determination of Currentâ^'Voltage Curves in Perovskite Solar Cells via Photoluminescence. Solar Rrl, 2021, 5, 2100348.	3.1	7

#	Article	IF	CITATIONS
19	Correction to "Boron Spin-On Doping for Poly-Si/SiOx Passivating Contacts― ACS Applied Energy Materials, 2021, 4, 6376-6376.	2.5	0
20	Contactless and Spatially Resolved Determination of Currentâ^'Voltage Curves in Perovskite Solar Cells via Photoluminescence. Solar Rrl, 2021, 5, 2170083.	3.1	1
21	Micro-photoluminescence studies of shallow boron diffusions below polysilicon passivating contacts. Solar Energy Materials and Solar Cells, 2021, 227, 111108.	3.0	2
22	Complementary bulk and surface passivations for highly efficient perovskite solar cells by gas quenching. Cell Reports Physical Science, 2021, 2, 100511.	2.8	21
23	Twist-driven wide freedom of indirect interlayer exciton emission in MoS2/WS2 heterobilayers. Cell Reports Physical Science, 2021, 2, 100509.	2.8	23
24	Combined Bulk and Surface Passivation in Dimensionally Engineered 2Dâ€3D Perovskite Films via Chlorine Diffusion. Advanced Functional Materials, 2021, 31, 2104251.	7.8	37
25	Zero-emission multivalorization of light alcohols with self-separable pure H2 fuel. Applied Catalysis B: Environmental, 2021, 292, 120212.	10.8	5
26	Impact of Gettering and Hydrogenation on Sub-Band-Gap Luminescence from Ring Defects in Czochralski-Grown Silicon. ACS Applied Energy Materials, 2021, 4, 11258-11267.	2.5	2
27	Investigation of Gallium–Boron Spinâ€On Codoping for poly‣i/SiO <sub><i>x</i></sub> Passivating Contacts. Solar Rrl, 2021, 5, 2100653.	3.1	3
28	Investigation of Gallium–Boron Spinâ€On Codoping for polyâ€&i/SiO <sub><i>x</i></sub> Passivating Contacts. Solar Rrl, 2021, 5, .	3.1	1
29	Hydrogenation in multicrystalline silicon: The impact of dielectric film properties and firing conditions. Progress in Photovoltaics: Research and Applications, 2020, 28, 493-502.	4.4	7
30	Hydrogenation Mechanisms of Poly‣i/SiO <sub><i>x</i></sub> Passivating Contacts by Different Capping Layers. Solar Rrl, 2020, 4, 1900476.	3.1	13
31	Spatially and Spectrally Resolved Absorptivity: New Approach for Degradation Studies in Perovskite and Perovskite/Silicon Tandem Solar Cells. Advanced Energy Materials, 2020, 10, 1902901.	10.2	9
32	Influence of PECVD deposition temperature on phosphorus doped poly-silicon passivating contacts. Solar Energy Materials and Solar Cells, 2020, 206, 110348.	3.0	24
33	Micro-photoluminescence studies of shallow phosphorus diffusions below polysilicon passivating contacts. Solar Energy Materials and Solar Cells, 2020, 218, 110780.	3.0	1
34	All-perovskite tandem solar cells with 24.2% certified efficiency and area over 1 cm2 using surface-anchoring zwitterionic antioxidant. Nature Energy, 2020, 5, 870-880.	19.8	497
35	In Situ Formation of Mixedâ€Dimensional Surface Passivation Layers in Perovskite Solar Cells with Dualâ€Isomer Alkylammonium Cations. Small, 2020, 16, e2005022.	5.2	34
36	A Correlative Study of Film Lifetime, Hydrogen Content, and Surface Passivation Quality of Amorphous Silicon Films on Silicon Wafers. IEEE Journal of Photovoltaics, 2020, 10, 1307-1312.	1.5	2

#	Article	IF	CITATIONS
37	Mechanisms and Applications of Steady-State Photoluminescence Spectroscopy in Two-Dimensional Transition-Metal Dichalcogenides. ACS Nano, 2020, 14, 14579-14604.	7.3	56
38	Deposition pressure dependent structural and optoelectronic properties of ex-situ boron-doped poly-Si/SiOx passivating contacts based on sputtered silicon. Solar Energy Materials and Solar Cells, 2020, 215, 110602.	3.0	17
39	Emission Control from Transition Metal Dichalcogenide Monolayers by Aggregation-Induced Molecular Rotors. ACS Nano, 2020, 14, 7444-7453.	7.3	23
40	Efficient Passivation and Low Resistivity for p <sup>+</sup> -Si/TiO <sub>2</sub> Contact by Atomic Layer Deposition. ACS Applied Energy Materials, 2020, 3, 6291-6301.	2.5	5
41	Hydrogenation Mechanisms of Poly‣i/SiO <sub><i>x</i></sub> Passivating Contacts by Different Capping Layers. Solar Rrl, 2020, 4, 2070033.	3.1	10
42	Supertransport of excitons in atomically thin organic semiconductors at the 2D quantum limit. Light: Science and Applications, 2020, 9, 116.	7.7	32
43	Tandem Solar Cells: Spatially and Spectrally Resolved Absorptivity: New Approach for Degradation Studies in Perovskite and Perovskite/Silicon Tandem Solar Cells (Adv. Energy Mater. 4/2020). Advanced Energy Materials, 2020, 10, 2070016.	10.2	0
44	Contactless, nondestructive determination of dopant profiles of localized boron-diffused regions in silicon wafers at room temperature. Scientific Reports, 2019, 9, 10423.	1.6	2
45	Modulated interlayer charge transfer dynamics in a monolayer TMD/metal junction. Nanoscale, 2019, 11, 418-425.	2.8	33
46	Solar Cells: Quantifying Quasiâ€Fermi Level Splitting and Mapping its Heterogeneity in Atomically Thin Transition Metal Dichalcogenides (Adv. Mater. 25/2019). Advanced Materials, 2019, 31, 1970180.	11.1	2
47	Multiwavelength Single Nanowire InGaAs/InP Quantum Well Light-Emitting Diodes. Nano Letters, 2019, 19, 3821-3829.	4.5	32
48	Quantifying Quasiâ€Fermi Level Splitting and Mapping its Heterogeneity in Atomically Thin Transition Metal Dichalcogenides. Advanced Materials, 2019, 31, e1900522.	11.1	34
49	Perovskite Solar Cells: Imaging Spatial Variations of Optical Bandgaps in Perovskite Solar Cells (Adv.) Tj ETQq1 1	0.784314 10.2	rgBT /Over
50	Predicting Open-Circuit Voltages in Atomically-Thin Monolayer Transition Metal Dichalcogenides-Based Solar Cells. , 2019, , .		0
51	Luminescence from poly-Si films and its application to study passivating-contact solar cells. , 2019, , .		0
52	Hydrogenation of polycrystalline silicon films for passivating contacts solar cells. , 2019, , .		2
53	Extracting optical bandgaps from luminescence images of perovskite solar cells. , 2019, , .		0
54	Light-activated inorganic CsPbBr <sub>2</sub> I perovskite for room-temperature self-powered chemical sensing. Physical Chemistry Chemical Physics, 2019, 21, 24187-24193.	1.3	23

Hieu T Nguyen

#	Article	IF	CITATIONS
55	Aluminium and zinc co-doped CuInS2 QDs for enhanced trion modulation in monolayer WS2 toward improved electrical properties. Journal of Materials Chemistry C, 2019, 7, 15074-15081.	2.7	12
56	Hydrogen-Assisted Defect Engineering of Doped Poly-Si Films for Passivating Contact Solar Cells. ACS Applied Energy Materials, 2019, 2, 8783-8791.	2.5	12
57	Hydrogenation of Phosphorus-Doped Polycrystalline Silicon Films for Passivating Contact Solar Cells. ACS Applied Materials & Interfaces, 2019, 11, 5554-5560.	4.0	47
58	Imaging Spatial Variations of Optical Bandgaps in Perovskite Solar Cells. Advanced Energy Materials, 2019, 9, 1802790.	10.2	18
59	Characterization of Epitaxial Heavily Doped Silicon Regions Formed by Hot-Wire Chemical Vapor Deposition Using Micro-Raman and Microphotoluminescence Spectroscopy. IEEE Journal of Photovoltaics, 2018, 8, 813-819.	1.5	3
60	Dynamically Gasâ€Phase Switchable Super(de)wetting States by Reversible Amphiphilic Functionalization: A Powerful Approach for Smart Fluid Gating Membranes. Advanced Functional Materials, 2018, 28, 1704423.	7.8	12
61	Reconstructing photoluminescence spectra at liquid nitrogen temperature from heavily boronâ€doped regions of crystalline silicon solar cells. Progress in Photovoltaics: Research and Applications, 2018, 26, 587-596.	4.4	4
62	Ring defects in n-type Czochralski-grown silicon: A high spatial resolution study using Fourier-transform infrared spectroscopy, micro-photoluminescence, and micro-Raman. Journal of Applied Physics, 2018, 124, 243101.	1.1	14
63	Modeling Photoluminescence Spectra in Heavily Boron Doped Silicon. , 2018, , .		0
64	Radial Growth Evolution of InGaAs/InP Multi-Quantum-Well Nanowires Grown by Selective-Area Metal Organic Vapor-Phase Epitaxy. ACS Nano, 2018, 12, 10374-10382.	7.3	26
65	Sub-Bandgap Luminescence from Doped Polycrystalline and Amorphous Silicon Films and Its Application to Understanding Passivating-Contact Solar Cells. ACS Applied Energy Materials, 2018, 1, 6619-6625.	2.5	18
66	Efficient and Layerâ€Dependent Exciton Pumping across Atomically Thin Organic–Inorganic Typeâ€I Heterostructures. Advanced Materials, 2018, 30, e1803986.	11.1	79
67	Detecting Dopant Diffusion Enhancement at Grain Boundaries in Multicrystalline Silicon Wafers With Microphotoluminescence Spectroscopy. IEEE Journal of Photovoltaics, 2017, 7, 598-603.	1.5	6
68	Photoluminescence Spectra of Moderately Doped, Compensated Silicon Si:P,B at 79–300 K. IEEE Journal of Photovoltaics, 2017, 7, 581-589.	1.5	6
69	Microscopic Distributions of Defect Luminescence From Subgrain Boundaries in Multicrystalline Silicon Wafers. IEEE Journal of Photovoltaics, 2017, 7, 772-780.	1.5	16
70	Activation Kinetics of the Boron–oxygen Defect in Compensated n- and p-type Silicon Studied by High-Injection Micro-Photoluminescence. IEEE Journal of Photovoltaics, 2017, 7, 988-995.	1.5	6
71	Growth of Oxygen Precipitates and Dislocations in Czochralski Silicon. IEEE Journal of Photovoltaics, 2017, 7, 735-740.	1.5	12
72	Precipitation of Cu and Ni in n- and p-type Czochralski-grown silicon characterized by photoluminescence imaging. Journal of Crystal Growth, 2017, 460, 98-104.	0.7	5

#	Article	IF	CITATIONS
73	Imaging the Thickness of Passivation Layers for Crystalline Silicon with Micronâ€Scale Spatial Resolution Using Spectral Photoluminescence. Solar Rrl, 2017, 1, 1700157.	3.1	3
74	Quantification of Sheet Resistance in Boronâ€Diffused Silicon Using Microâ€Photoluminescence Spectroscopy at Room Temperature. Solar Rrl, 2017, 1, 1700088.	3.1	6
75	Light and Electrically Induced Phase Segregation and Its Impact on the Stability of Quadruple Cation High Bandgap Perovskite Solar Cells. ACS Applied Materials & Interfaces, 2017, 9, 26859-26866.	4.0	114
76	Optical Evaluation of Silicon Wafers With Rounded Rear Pyramids. IEEE Journal of Photovoltaics, 2017, 7, 1596-1602.	1.5	10
77	Interface passivation using ultrathin polymer–fullerene films for high-efficiency perovskite solar cells with negligible hysteresis. Energy and Environmental Science, 2017, 10, 1792-1800.	15.6	381
78	On the composition of luminescence spectra from heavily doped p-type silicon under low and high excitation. Journal of Luminescence, 2017, 181, 223-229.	1.5	11
79	Determination of Dopant Density Profiles of Heavily Boron-Doped Silicon From Low Temperature Microphotoluminescence Spectroscopy. IEEE Journal of Photovoltaics, 2017, 7, 1693-1700.	1.5	7
80	Evaluating Depth Distributions of Dislocations in Silicon Wafers Using Micro-Photoluminescence Excitation Spectroscopy. Energy Procedia, 2016, 92, 145-152.	1.8	2
81	Silicon Luminescence Spectra Modelling and the Impact of Dopants. Energy Procedia, 2016, 92, 852-856.	1.8	0
82	Characterization of Cu and Ni Precipitates in n– and p-type Czochralski-grown Silicon by Photoluminescence. Energy Procedia, 2016, 92, 880-885.	1.8	1
83	Quantifying boron and phosphorous dopant concentrations in silicon from photoluminescence spectroscopy at 79 K. Physica Status Solidi (A) Applications and Materials Science, 2016, 213, 3029-3032.	0.8	9
84	Structural engineering using rubidium iodide as a dopant under excess lead iodide conditions for high efficiency and stable perovskites. Nano Energy, 2016, 30, 330-340.	8.2	133
85	Low-temperature micro-photoluminescence spectroscopy on laser-doped silicon with different surface conditions. Applied Physics A: Materials Science and Processing, 2016, 122, 1.	1.1	8
86	Photoluminescence Excitation Spectroscopy of Diffused Layers on Crystalline Silicon Wafers. IEEE Journal of Photovoltaics, 2016, 6, 746-753.	1.5	6
87	Characterizing amorphous silicon, silicon nitride, and diffused layers in crystalline siliconsolarcellsusingmicro-photoluminescence spectroscopy. Solar Energy Materials and Solar Cells, 2016, 145, 403-411.	3.0	18
88	Effects of Solar Cell Processing Steps on Dislocation Luminescence in Multicrystalline Silicon. Energy Procedia, 2015, 77, 619-625.	1.8	7
89	Uncertainty analysis for the coefficient of band-to-band absorption of crystalline silicon. AIP Advances, 2015, 5, .	0.6	313
90	Dislocations in laser-doped silicon detected by micro-photoluminescence spectroscopy. Applied Physics Letters, 2015, 107, .	1.5	27

#	Article	IF	CITATIONS
91	Experimental Determination of the Uncertainty of the Absorption Coefficient of Crystalline Silicon. Energy Procedia, 2015, 77, 170-178.	1.8	4
92	Microâ€photoluminescence spectroscopy on heavilyâ€doped layers of silicon solar cells. Physica Status Solidi - Rapid Research Letters, 2015, 9, 230-235.	1.2	28
93	Micrometer-Scale Deep-Level Spectral Photoluminescence From Dislocations in Multicrystalline Silicon. IEEE Journal of Photovoltaics, 2015, 5, 799-804.	1.5	29
94	Ultralow Absorption Coefficient and Temperature Dependence of Radiative Recombination of CH <sub>3</sub> NH <sub>3</sub> PbI <sub>3</sub> Perovskite from Photoluminescence. Journal of Physical Chemistry Letters, 2015, 6, 767-772.	2.1	73
95	Impact of Carrier Profile and Rear-Side Reflection on Photoluminescence Spectra in Planar Crystalline Silicon Wafers at Different Temperatures. IEEE Journal of Photovoltaics, 2015, 5, 77-81.	1.5	15
96	Temperature dependence of the band-band absorption coefficient in crystalline silicon from photoluminescence. Journal of Applied Physics, 2014, 115, .	1.1	80
97	Temperature dependence of the radiative recombination coefficient in crystalline silicon from spectral photoluminescence. Applied Physics Letters, 2014, 104, .	1.5	58